BayesShrink Ridgelets for Image Denoising

Nezamoddin Nezamoddini-Kachouie, Paul Fieguth, and Edward Jernigan

University of Waterloo, Department of Systems Design Engineering, Waterloo, Ontario, N2L 3G1, Canada
{nnezamod, pfieguth, jernigan}@uwaterloo.ca
ocho.uwaterloo.ca

Abstract. The wavelet transform has been employed as an efficient method in image denoising via wavelet thresholding and shrinkage. The ridgelet transform was recently introduced as an alternative to the wavelet representation of two dimensional signals and image data. In this paper, a BayesShrink ridgelet denoising technique is proposed and its denoising performance is compared with a previous VisuShrink ridgelet method. To derive the results, different wavelet bases such as Daubechies, symlets and biorthogonal are used. Experimental results show that BayesShrink ridgelet denoising yields superior image quality and higher SNR than VisuShrink.

1 Introduction

Data obtained from the real world in the form of signals do not exist without noise. This noise might decrease to some negligible levels under ideal conditions such that denoising is not necessary, but usually to recover the signal the corrupting noise must be removed for practical purposes. For this reason noise elimination is a main concern in computer vision and image processing. Noise undesirably corrupts the image by perturbations which are not related to the scene under study and ambiguates the underlying signal relative to its observed form.

The goal of denoising is to remove the noise and to retain the important signal features as much as possible. To achieve this goal, traditional approaches use linear processing such as Wiener filtering. In the presence of additive noise, linear filters, which consist of convolving the image with a constant matrix to obtain a linear combination of neighborhood values, can produce a blurred and smoothed image with poor feature localization and incomplete noise suppression. To overcome this shortcoming, nonlinear filters have been proposed. Much research has focused recently on signal denoising using nonlinear techniques; of which one of the most important is wavelet based denoising. The wavelet transform generally separates signal and noise; as a result it can be used to remove the noise while preserving the signal characteristics. Researchers have employed various approaches to nonlinear wavelet-based denoising: In one approach, wavelet thresholding, a hard threshold function keeps a coefficient if it is larger than a threshold and sets it to zero otherwise; in another,

A. Campilho, M. Kamel (Eds.): ICIAR 2004, LNCS 3211, pp. 163–170, 2004.

wavelet shrinkage takes the coefficient and shrinks it toward zero by some threshold. Both approaches are nonlinear and operate on one wavelet coefficient at a time.

Recently the Ridgelet and Curvelet transforms were developed to reduce the limitations of wavelet-based image processing. The two-dimensional wavelet image transform produces large coefficients along important edges even at fine scales. Hence, edges of an image appear as large wavelet coefficients repeatedly at fine scales, so to properly reconstruct the edges of the image many wavelet coefficients are required. The estimation of so many coefficients makes wavelet denoising techniques complex.

On the other hand, wavelet transforms can catch the point singularities of one-dimensional (1-D) signals, thus they have a good performance for one-dimensional smooth functions. To discover 1-D singularities in two-dimensional (2-D) signals, the wavelet transform faces some difficulties. Images that contain 2-D smooth signals have 1-D singularities across the edges which separate the smooth regions. Although edges are generally smooth curves, as borders of two smooth regions they are discontinues. Since the 2-D wavelet transform is the product of 1-D wavelets, it discovers the singularities across the edges but it doesn't recognize the smoothness along the edges. To compensate for this weakness of the wavelet transform in higher dimensions, ridgelet and curvelet transforms were recently introduced by Candes and Donoho [1-4].

Different denoising methods have been proposed for signal denoising via wavelet. On the other hand VisuShrink ridgelet thresholding has been recently introduced [5] as an alternative to the wavelet denoising and performs better than wavelet for the images with straight lines. In this paper BayesShrink ridgelet image denoising is proposed and the results are compared with those of VisuShrink ridgelet method. The following Section explains rigelet image denoising. In Section three ridgelet thresholding techniques are described. The proposed method is presented in Section four. In Section five the results of the proposed method and the previous VisuShrink technique are compared and the conclusions are presented in Section 6.

2 Ridgelet Image Denoising

The ridgelet transform was proposed as an alternative to the wavelet transform to represent 2-D signals. Since a sparse representation of smooth functions and straight edges is provided by the ridgelet transform, this new expansion can accurately represent both smooth functions and edges with a few nonzero coefficients and achieves a lower mean square error (MSE) than the wavelet transform.

2.1 Ridgelet Transform

The ridgelet transform effectively represents line singularities of 2-D signals. It maps the line singularities into point singularities in the Radon domain by employing the embedded Radon transform. Therefore, the wavelet transform can efficiently be ap-

plied to discover the point singularities in this new domain. Having the ability to approximate singularities along a line, several terms with common ridge lines can effectively be superposed by the ridgelet transform. The bivariate ridgelet transform in R^2 is defined by:

$$\Re_{\alpha,\beta,\theta}(\kappa) = \alpha^{-1/2}\omega((\kappa_1 \cos\theta + \kappa_2 \sin\theta - \beta)\ /\alpha) \tag{1}$$

where ω is a univariate wavelet function on $R \rightarrow R$. $\alpha > 0$, β and θ are scale, location and orientation parameters respectively. Along the ridgelet lines $\kappa_1 \cos\theta + \kappa_2 \sin\theta$, ridgelets are constant and they are equal to the wavelets in the orthogonal direction. ridgelet coefficients of a bivariate function $I(\kappa)$ in R^2 are given by:

$$\Re_I(\alpha,\beta,\theta) = \int \Re_{\alpha,\beta,\theta}\ (\kappa) I(\kappa) d\kappa \tag{2}$$

The reconstruction formula is given by:

$$I(\kappa) = \int_0^{2\pi} \int_{-\infty}^{+\infty} \int_0^{\infty} \Re_I(\alpha,\beta,\theta)\, \Re_{\alpha,\beta,\theta}\ (\kappa) \frac{d\alpha}{\alpha^3} d\beta \frac{d\theta}{4\pi} \tag{3}$$

and is valid for integrable (and square integrable) functions. Like Fourier and wavelet transforms, any arbitrary function can be represented by continuous superposition of ridgelets. Considering the 2-D ridgelet transform as a 1-D wavelet transform in the Radon domain, the ridgelet coefficients of function $I(\kappa)$ can be defined as:

$$\Re_I(\alpha,\beta,\theta) = \int \Re_t(\theta,\tau)\alpha^{-1/2}\omega((\tau-\beta)/\alpha) d\tau \tag{4}$$

where $R_t(\theta,t)$ is the Radon transform of function $I(\kappa)$ and is given based on the Dirac distribution (δ) as:

$$\Re_t(\theta,\tau) = \int I(\kappa_1,\kappa_2)\delta(\kappa_1 \cos\theta + \kappa_2 \sin\theta - \tau) d\kappa_1 d\kappa_2 \tag{5}$$

2.2 Ridgelet Denoising Concept

To explain the ridgelet denoising procedure, assume *I[i,j]* to be the original *M* by *M* image, where *i and j = 1, 2,..., M*, and *S[i,j] = I[i,j] + n[i,j]* is the image corrupted by additive noise *n[i,j]* which is identically distributed and independent of *I[i,j]*. In the first step of ridgelet denoising, the observed image *S* is transformed into the ridgelet domain. Then the ridgelet coefficients are thresholded and finally the denoised coefficients are transformed back to reconstruct the image. Let R_D and R_R be the forward ridgelet decomposition and inverse ridgelet reconstruction transforms. Assume *T* and τ to be the thresholding operator and threshold respectively. The ridgelet thresholding can be summarized as:

$$(i)\ I_R = R_D(I),\ (ii)\ I_T = T(I_R,\ \tau),\ and\ (iii)\ \hat{I} = R_R I_\tau$$

The choice of the threshold and the method which is used to calculate the threshold, determine how efficient the denoising technique would be. Although selecting a small threshold may produce an output image close to the input, the recovered image may still be noisy. On the other hand, a choice of a large threshold may yield a blurred image by setting most of the wavelet coefficients to zero. Two different thresholding techniques, VisuShrink and BayesShrink, are explained in the following Section.

3 Thresholding Techniques

The ridgelet denoising is used to recover the original signal from the noisy one by removing the noise. In contrast with denoising methods that simply smooth the signal by preserving the low frequency content and removing the high frequency components, the frequency contents and characteristics of the signal would be preserved during ridgelet denoising.

3.1 VisuShrink

VisuShrink, proposed by Donoho and Johnstone [6,9], uses the universal threshold given by:

$$U_t = \sigma_n \sqrt{2 \log M} \tag{6}$$

where σ_n and M are the noise variance and the number of image pixels respectively. Donoho and Jonstone have proved [6-8] that the maximum of any M independent and identically distributed (iid) values with high probability is less than the universal threshold U_t. As M is increased the probability will be closer to one, so with a high probability pure noise signals are set to zero. Since the universal threshold is obtained by considering the constraint that the noise is less than the threshold with high probability as M increases, it tends to be high for large values of M and as a result will shrink many noisy ridgelet coefficients to zero and produce smoothed estimated images.

3.2 BayesShrink

As it was suggested for the subband wavelet coefficients by [10,11], the subband ridgelet coefficients of a natural image can also be described by the Generalized Gaussian Distribution (GGD) as:

$$GG_{\sigma_I,\gamma}(I) = P(\sigma_I, \gamma) \exp\{-[\delta(\sigma_I, \gamma) \mid I \mid]^{\gamma}\} \tag{7}$$

where $-\infty < I < +\infty$, $\gamma > 0$ and,

$$\delta(\sigma_I, \gamma) = \sigma_I^{-1}\left[\frac{\Gamma(3/\gamma)}{\Gamma(1/\gamma)}\right]^{\frac{1}{2}} \tag{8}$$

and,

$$P(\sigma_I, \gamma) = \frac{\gamma \bullet \delta(\sigma_I, \gamma)}{2\Gamma\left(\frac{1}{\gamma}\right)} \tag{9}$$

σ_I is the standard deviation of subband ridgelet coefficients, γ is the shape parameter and Γ is Gamma function. For most natural images the distribution of the ridgelet coefficients in a subband can be described with a shape parameter γ in the range of [0.5,1]. Considering such a distribution for the ridgelet coefficients and estimating γ and σ_I for each subband, the soft threshold T_S which minimizes the Bayesian Risk [10,11], can be obtained by:

$$\Re(T_S) = E(\hat{I} - I)^2 = E_I E_{J|I}(\hat{I} - I)^2 \tag{10}$$

where $\hat{I}$ is $T_S(J)$, $J|I$ is $N(I,\sigma)$ and I is $GG_{\sigma_I,\gamma}$. Then the optimal threshold T_S^* is given by:

$$\mathrm{T}_\mathrm{S}^*(\sigma_\mathrm{I}, \gamma) = \arg\min_{T_S} \Re(T_S) \tag{11}$$

Numerical calculation is used to find T_S^* since it does not have a closed form solution. A proper estimation of the value T_S^* is concluded by setting the threshold as [10,11]:

$$\hat{T}(\hat{\sigma}_I) = \frac{\hat{\sigma}_n}{\hat{\sigma}_I} \tag{12}$$

4 Calculating the BayesShrink Threshold by the Proposed Method

Subband dependent threshold is used to calculate BayesShrink ridgelet threshold. The estimated threshold is given by (12) where σ_n and σ_I are noise and signal standard deviations respectively. The 1-D ridgelet coefficients corresponding to different directions are depicted in Fig. 1. In this figure each column corresponds to a specific direction, hence the number of columns determines the number of directions and each column contains subband detail coefficients for L different decomposition levels.

To estimate the noise variance σ_n^2 from the subband details, the median estimator is used on the 1-D subband coefficients:

$$\hat{\sigma}_n = median(|Details|)/0.6745 \tag{13}$$

Signal standard deviation is calculated for each direction in each subband detail individually. Thus having *N* directions and *L* subband, *NxL* different σ_I must be estimated corresponding to *NxL* subband-directions coefficients. Note that in BayesShrink wavelet denoising, σ_I is estimated on 2-D dyadic subbands [10,11]. Thus having *L* decomposition levels, *3xL* different σ_I must be estimated to calculate the thresholds for the different subbands. To estimate the signal standard deviation *(*σ_I*),* the observed signal *S* is considered to be $S = I + n$ and signal *(I)* and noise *(n)* are assumed to be independent. Therefore,

$$\sigma_S^2 = \sigma_I^2 + \sigma_n^2 \tag{14}$$

where σ_S^2 is the variance of the observed signal. So $\hat{\sigma}_I$ is estimated by:

$$\hat{\sigma}_I = \sqrt{\max((\hat{\sigma}_S^2 - \hat{\sigma}_n^2),0)} \tag{15}$$

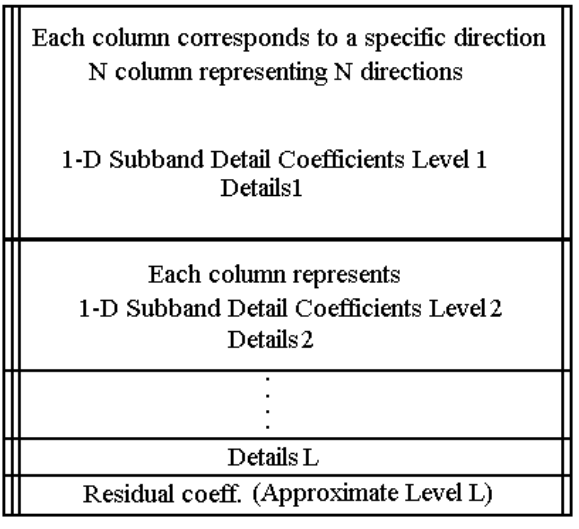

Fig. 1. Subband ridgelet coefficients: *N* directions (columns) and *L* levels which conclude *NxL* subband-direction coefficients

5 Results

In this section the proposed ridgelet denoising technique is used to recover the noisy images which are corrupted with additive white noise. BayesShrink and VisuShrink ridgelet image denoising methods are implemented and based on different wavelet bases the results are compared. Since the ridgelet transform performs better on images with straight lines, the test image in the following experiments, as depicted in Fig. 2, is an image with perfectly straight lines which has been used in [5]. Denoised images depicted in Fig. 2(c1)-2(e1) and 2(c2)-2(e2) are derived using the BayesShrink and VisuShrink thresholding methods respectively. The results are obtained based on

three different wavelet bases including Daubechies, Symlets and Biorthogonal. As we can observe according to the SNR measurements, the results obtained by BayesShrink ridgelet method are better than those obtained by VisuShrink ridgelet method using different wavelet bases. On the other hand based on image quality BayesShrink provides superior results than VisuShrink. Therefore, regardless of the wavelet bases BayesShrink ridgelet provides better performance than VisuShrink ridgelet denoising.

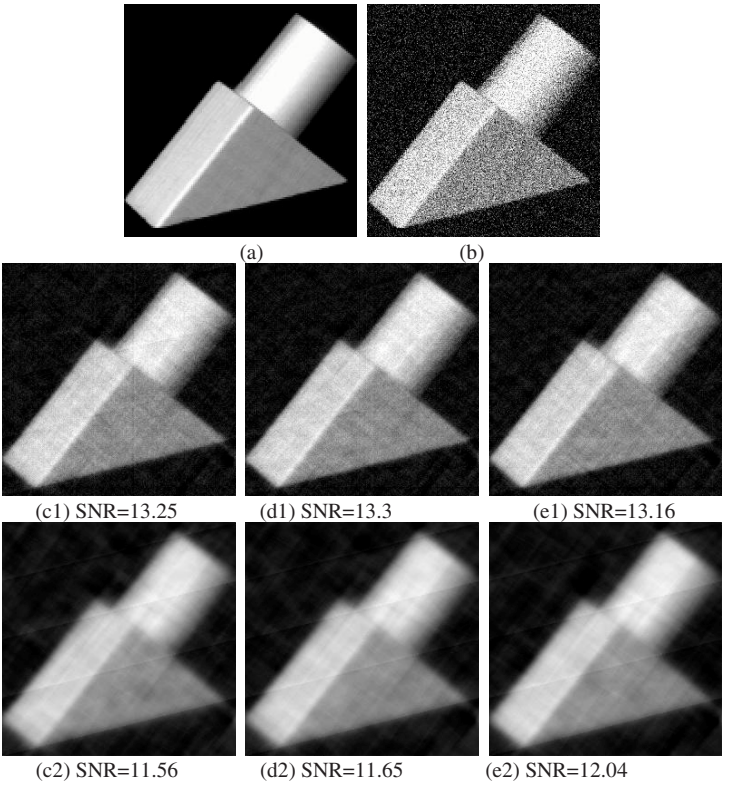

Fig. 2. (a) Original Image. (b) Noisy Image with SNR = 7.22. BayesShrink Ridgelet Denoising: (c1) db4. (d1) sym8. (e1) bior3.9. VisuShrink Ridgelet Denoising: (c2) db4. (d2) sym8. (e2) bior3.9.

6 Conclusions

In this paper the ridgelet transform for image denoising was addressed. BayesShrink ridgelet denoising was proposed. The proposed method was applied on test images with perfectly straight lines. The denoising performance of the results was compared with that of the VisuShrink ridgelet image denoising method. The experimental results by the proposed method showed the superiority of the image quality and its higher SNR in comparison with VisuShrink ridgelet technique. Furthermore we ob-

served that regardless of the selected wavelet basis, BayesShrink ridgelet performs better than VisuShrink ridgelet denoising method. However, the choice of the wavelet bases might affect the performance of both methods.

Future work is needed to improve the performance of this method. The BayesShrink curvelet denoising would also be compared with BayesShrink ridgelet denoisisng method. Moreover, the effect of the wavelet bases and the number of the decomposition levels on the performance of the denoised images would be investigated based on wavelet, ridgelet and curvelet methods.

References

1. Candes, E. J.: Ridgelets: Theory and Applications, Ph.D. thesis, Department of Statistics, Stanford University (1998)
2. Candes, E. J., Donoho, D. L.: Ridgelets: a key to higher dimensional intermittency?, Phil. Trans. R. Soc. Lond. A. (1999) 2495-2509
3. Donoho, D. L., Duncan, M. R.: Digital Curvelet Transform: Strategy, Implementation and Experiments, Proc.SPIE, Vol. 4056 (2000) 12-29
4. Starck, J. L., Candes, E. J., Donoho, D. L.: The Curvelet Transform for Image Denoising, IEEE Tran on Image Processing, Vol. 11, No. 6 (2002) 670-684
5. Do, M. N., Vetterli, M.: The Finite Ridgelet Transform for Image Representa tion, IEEE Tran. on Image Processing, Vol. 12, No.1 (Jan. 2003) 16 – 28
6. Donoho, D. L., Johnstone, I. M.: Ideal Spatial Adaptation via wavelet Shrinkage, Biometrika, Vol. 81 (Sept. 1994) 425-455
7. Donoho, D. L., Johnstone, I. M.: Adapting to Unknown Smoothness via Wavelet Shrinkage, Biometrika, Vol. 81 (Sept 1994) 425-455
8. Donoho, D. L.: Denoising by Soft Thresholding, IEEE Tran. on Inf. Theory, Vol. 41 (May1997) 613-627
9. Taswell, C.: The What, How, and Why of Wavelet Shrinkage Denoising, IEEE Journal Computing in Science and Engineering, Vol. 2, No. 3. (May-June 2000) 12-17
10. Chang, S. G., Yu, B., Vetterli, M.: Adaptive Wavelet Thresholding for Image Denoising and Compression, IEEE Trans. on Image Processing, Vol. 9, No. 9 (2000) 1532-1546
11. Chang, S. G., Yu, B., Vetterli, M.: Spatially Adaptive Wavelet Thresholding with Context Modeling for Image Designing, IEEE Tran on Image Processing, Vol. 9, No. 9 (2000) 1522-1531